International Journal of Innovative Research in Engineering & Management (IJIREM)
ISSN: 2350-0557, Volume-3, Issue-3, May-2016

Selectivity Modeling of Fischer-Tropsch Synthesis over Fe-Mn Catalyst Using Artificial Neural Networks

Hossein. Atashi[1], Neda. Poudineh[2], Amin. Ein Beigi[3]
[1, 2, 3]Department of Chemical Engineering Faculty of Engineering,
University of Sistan and Baluchestan,
P.O.Box 98164-161,
Zahedan,Iran.

ABSTRACT
The Fischer-Tropsch synthesis is the collection of several reactions which are used to produce hydrocarbon products from synthesis gas. This method is able to produce more than 70 types of products. The selectivity models of the products such as: diesel, gasoline, methane and C_{21}^{+}in the Fischer-Tropsch synthesis over Fe-Mn catalyst were obtained while have been discussed less about the selectivity models in the references. Neural networks and response surface method were used to determine the effect of operating parameters such as: temperature, pressure and H_2/CO ratio and space velocity on the selectivity of products. Operating parameters were varied as follow: reaction temperature 523-573 K, reaction pressure 1.5-3 Mpa and H_2/CO ratio 0.67-2. The highest influence related to temperature and H_2/CO ratio parameters and the lowest was pressure on the selectivity of products such that has been removed from some of the models.
In addition, the interaction between temperature and H_2/CO ratio was interaction parameter. The results showed that the values predicted by the neural network could satisfy the experimental data, so use of neural network to predict the selectivity values in Fischer-Tropsch synthesisis an effective method.

Keywords: Artificial neural networks, Fischer-Tropsch synthesis, Fe-Mn catalyst, selectivity, Response surface model

1. INTRODUCTION
Decreasing oil resources and the existence of high resource of methane and coal (1.5 and 25 times of that of the crude oil) and also increasing petroleum price in recent decades caused to considered the Fischer- Tropsch Synthesis (FTS) significantly [1-5]. In FT reaction, synthesis gas (CO and H2) convert into paraffin's, olefins and oxygenated compounds [1, 6-10]. All of these products are resulted from hydrogenation and polymerization of carbon monoxide [11]. Converting of Syngas is perform at two procedures, low temperature and high temperature that high temperature is mainly used to convert gasoline and chemicals like alpha-olefins and low temperature method is appropriate for the production of waxes [12]. Catalyst plays an importance role in the FT process. Between all metals which can be used to provide the required activity of FT process, Iron and Cobalt catalysts have been more
Studied and used for industrial applications [13, 14].
Iron-based catalyst system (namely Fe-Cu-K and Fe-Mn catalysts) is highly regarded because of several reasons such as: low cost and high water-gas shift reaction. Also the iron-based catalysts are more appropriate for synthesis gas rich in CO [15-19] and have high efficiency of olefin in the distribution of hydrocarbons [20-25]. Some of metals such as K, Mn, Cu, and Ca can be used as promoters for improving Fe-based catalyst performance [26]. Recently, the catalytic system of iron-manganese has been highly considered since the properties such as: high selectivity of alkenes with low molecular weight [27-29], high selectivity of middle distillate cut products (these products derived from it, can be used as feedstock of chemical industrial) and increasing FTS activity [30-33]. Selection of an appropriate reactor is another significant subject in the FT process. Among all reactors that have been used in this industry (fixed bed, fluidized bed reactors and slurry bubble column reactor), the slurry bubble column reactors (SBC) have special importance [3, 7]. Since the FT process is a highly-exothermic process (Hr = -165Kj/mol) [11] Thus, slurry bubble column reactors are considered an appropriate choice for this process due to many advantages such as: temperature proper control and the small size of solid particles which leads to higher efficiency, low pressure drop, its low operation cost, low constructions [1, 34] and a relatively high coefficient of heat transfer [30, 33].
In addition to the mentioned cases, it is important to obtain models which can offer manner of distribution of FT products since in FT reaction produced over 70 different products. On other hand, studying and finding the best operating conditions that can support maximum production of designed products is costly and time consuming. Therefore trying to reduce the costs and save time while achieving favorable results is an important matter.
Selectivity models are convenient and practical ways for explain how the distribution of any of products during reaction. It also investigate the effect of each operating parameters (temperature, pressure, space velocity and H2/CO ratio in feed) and the impact of interaction of them. In this study, selectivity models of products of FTS, the performance of these effective parameters on the selectivity of the products and their effects on each other are evaluated using artificial neural network (ANN) and response surface model (RSM).

1.1. Artificial Neural Network (ANN)

In recent years, ANN have been identified an appropriate strategy and applications to improve the experimental models by means of modeling [35]. ANN is made of a genetics algorithm. Actually is a calculated model that has been grounded on the basis of processor system of human brain data and is considered as one of the useful optimization methods to get the best input and output for a system. Knowledge of neural networks is achieved from patterns and relationship between the empirical data that is used to its education [36-39].

Complex and non-linear issues are simulated with using a different number of these non-linear processing elements [40]. ANN is set of layers and nodes or neurons (processing elements). These layers are divided into three categories: input layer (receiver of raw data), the output layer (its performance is depending on the hidden layer activity and neurons weight) and the middle layer (the layer where data processing is carried out) [41, 42]. Neurons are powerful, small, single (but related to each other) processor elements [43]. They are connected to each other by communications signal. Several inputs enter to each neuron from other neurons according to their weight and single output or multiple output signals are produced by each neuron [44]. The number of neuron is different for each layer so that, in the input layer, it is equal to the number of input parameters and for output layer is equal to the number of output parameters. For middle layer, which can also be formed from multiple layers, the number of nodes is also variable and depends on the achievement to the best response that is defined during simulation by the user. Each input elements multiplied on corresponding its weight when enters into a layer and connects with neurons. In other words, the training process of network is setting the neurons weights in response to the calculated error between calculated values and target value. Generally, neural network can be used in FT process as a predictor. Meaning that artificial neural network plays a role of a reactor in this matter (according to the definition given to it) i.e. by having experimental data on the defined operating conditions, they are used with the aim of training, validating and testing network and finally the required output data, which are dependent parameters, are calculated with very high accuracy.

2. EXPERIMENTS

In this study the selectivity models obtained from the data of referenced article [45], to FT products such as gasoline, diesel, methane and C_{21}^{+} (table 1).

This process carried out on Fe-Mn catalyst in the slurry column reactor with height and diameter 30 m and 5 m, respectively. The catalyst specifications are presented in table 2.

3. ARTIFICIAL NEURAL NETWORK-BASED MODELING

In order to selectivity modeling using ANN, temperature, pressure and H_2/CO ratio considered as independent variable (input data) and selectivity value of each products selected as depend variable (responses). The structure of the designed network in this paper is as follows (Figure 1):

ANN model was performed by using Matlab2012 Neural Network Module. Table 3 reported the calculated valid output data (responses).

The number of hidden layer (it is same number of used neurons) and output layers were 5 and 1, respectively.70% of the total input data were selected completely random by the neural network (data set) for training network, 15% for validation and 15% remained for the final test of the network's training. Levenberg- Marquart algorithm is a network training function that weight and bias values updates according to the optimization method of Levenberg- Marquart that was considered as learning algorithm for this neural network. The appropriate number of neurons in the middle layer was chosen 5 neurons. The best regression for each of the network parameters, such as: training, validation and testing are shown in Fig. 2 and table 4. Then a completely random experimental design was performed by RSM for each of the independent parameters in defined levels.

By entering obtained input from experimental design to trained network, the output (selectivity of each product) was calculated. Finally, selectivity models of products achieved by entering the response in the RSM.

4. RESULT AND DISCUSSION

As mentioned above, the selectivity model for each of the products of FTS such as: diesel, gasoline, methane and C_{21}^{+} were achieved by neural network and RSM.

Moreover, the effect of each of operating parameters on the products selectivity were investigated using ANOVA analysis, the ineffective parameters was removed from the model as for the P-values related to each of them. The Radj and R^2 are also provided before and after correction of the models and finally, the best model was presented for each of the products (tables 6-9).

On the other hand, optimal tools have been used to achieve optimum condition. The results are shown in Table 5.

The result showed a good agreement between predicted values with experimental data by comparing between them (Figs 3, 4 and 5). All regressions and statistical analysis was carried out by design -expert software version 7.

In order to investigate the impact of operating parameters and their interaction on selectivity of products, these selectivity models are reported in two ways: basic selectivity model and modified selectivity model (table 6-9).

In fact, by investigation the P-values of any of operating parameters and interaction parameters in basic selectivity models, the ineffective parameters were detected then by removing them from these models, the modified selectivity models were achieved. Furthermore the statistical indicators obtained for any of selectivity models are reported in these tables. As seen, all models with P-value <0.0001 were able to predicted the selectivity value of any of products with an accuracy of over 95% confidence.

Temperature, pressure and H_2/CO ratio operating parameters were effective on the selectivity of CH_4 and C_{21}^{+} while on selectivity of gasoline temperature and H_2/CO ratio and on distribution process of diesel two parameters temperature and pressure were more effective, respectively. The impact of interaction parameters on selectivity of products were more varied. So that the N×T, T_2, N_2 and P×T were more effective on the selectivity of two products CH_4 and C_{21}^{+}. But for gasoline N, T_2 and N_2 were only influential interaction parameters and P_2, P×N and P×T were removed from basic selectivity model of gasoline. The how influence of each interaction parameters on diesel selectivity is as follow:

T_2> N_2> N×T.

It should be mentioned that in this model H_2/CO ratio parameters with P-value equal to 0.418 remained in the modified selectivity model since it has an interaction effect on temperature parameter.

Evaluated impact of each operating condition on the selectivity of the products during the FT process is provided Fig. 6 (6a, 6b, 6c and 6d). For more details of comparison between the results of these graphs, all of these graphs are drawn based on two operating parameters, temperature and H_2/CO ratio, at a constant pressure of 2.5 MPa. According to consideration, among other interaction parameters, T×N, among all four models is the most effective. Figs. 6a and 6c showed alterations of the selectivity of the two products diesel and gasoline under the influence of changes of H_2/CO ratio and temperature at constant pressure 2.5 MPa. Both graphs shows similar results. As concluded from statistical results, the selectivity of these two products are a function of temperature, pressure and H_2/CO ratio in feed. This means that for middle distillate products with increasing temperature and H_2/CO ratio, at constant pressure, the selectivity increase and then began to decrease after reaching the maximum area.

The increase and decrease is a result of increasing temperature in low H_2/CO ratio within the reactor, for gasoline and diesel are 1.5 and 1.25 respectively, Due to the increase in carbon monoxide conversion, the production of longer-chain hydrocarbons and increases selectivity of these two products. But in the higher H_2/CO ratio, since hydrogen is not able to grow hydrocarbon chain by itself, the selectivity of these products decrease. Also, the reason of decreasing C_{21}^+selectivity and increasing CH_4 selectivity by increasing the temperature and the H_2/CO ratio can also be well understood by the same reason. (Figs. 6b and 6d). The Fig. 4 shows the changes of selectivity of each product by increasing pressure. Increasing pressure lead to increase long- chain hydrocarbons production. In fact smaller chains lead to produce larger chains. Hence the selectivity of CH_4 decrease. But at higher pressures because the production of hydrocarbons are beyond the range of C_{21}^+ while the amount of the input feed remains without change so, the amount of production of intermediate products decreases while the amount of C_{21}^+ selectivity continues dramatically to its increase. in addition to the experimental data, other results was calculated by neural network, that were calculated in the operating conditions defined by the experimental design (The operating conditions are within the range of operating conditions of laboratory), Thus were provided a wider possibility to predict the effect and importance of each operating parameter on the selectivity of the products more accurately.

5. CONCLUSION

In this study, the selectivity models were obtained with excellent accuracy, for products methane, diesel, gasoline and C_{21}^+ in the FTS over Fe-Mn catalyst by combining neural networks and experimental design. The simultaneous use of these software's led to additional examining of the applicability and possibility of using neural network to predict the selectivity of the FTS products. The impact of various operating parameters and interactions of these parameters on each other has better considered using neural network. According to the results, it was observed that of all the input parameters, H_2/CO ratio parameter at first priority and then the temperature in the second priority and also of all interaction parameters T×N (temperature- H_2/CO ratio) is influential parameters during the process. Also according to the calculated optimum conditions, the maximum amounts for the selectivity of each product were obtained as follows:

1- For diesel: 25.03 at P=1.5 MPa, H_2/CO=1.64 and T=559.87 K

2- For gasoline: 37.84 at P=1.5 MPa, H_2/CO=1.88 and T=545.22 K

3- For C_{21}^+: 67.08 at P=3.24 MPa, H_2/CO=0.67 and T=523 K

4- For CH_4: 67.05 at P=1.2 MPa, H_2/CO=2 and T=523 K

According to the comparison was performed between results from the neural network prediction and experimental data, selectivity models of products were obtained with very low error with the concomitant use of neural networks and experimental design. Finally, it must be pointed that achieving the selectivity models leads to decrease costs of experimental and saving time.

Acknowledgments

The authors would like to acknowledge the financial and instrumental supports from the University of Sistan and Baluchestan, Iran.

REFERENCES

[1] Dry ME. 2002. The Fischer–Tropsch process: 1950–2000. Catal Today. 71, 227-241. DOI= doi: 10.1016/S0920 5861(01)00453-9.

[2] Campos, A., Lohitharn, N., Roy, A., et al. 2010. An activity and XANES study of Mn-promoted, Fe-based Fischer–Tropsch catalysts. Appl Catal A: G. 375, 12-16. DOI= doi:10.1016/j.apcata.2009.11.015.

[3] Hoon, Yanga, J., Gul Hurc, Y., Hyun Chuna, D., et al. 2013. Hydrodynamic effect of oxygenated byproduct during Fischer–Tropsch synthesis in slurry bubble column. Chem Eng Proc 66: 27-35. DOI=doi:10.1016/j.cep.2013.01.007.

[4] van Vliet Oscar, P.R, Faaij André, P.C., Turkenburg Wim C. 2009. Fischer–Tropsch diesel production in a well-to-wheel perspective: A carbon, energy flow and cost analysis. Energy Convers Manage. 50, 855–876. DOI=doi:10.1016/j.enconman.2009.01.008.

[5] Schulz, H., 1999. Short history and present trends of Fischer–Tropsch synthesis. Appl Catal A: G. 186, 3-12.DOI= doi: 10.1016/S0926-860X (99)00160-X.

[6] Dry, ME., Hoogendoorn, JC. 1982. Hydrogenation of Carbon Monoxide Technology of the Fischer-Tropsch Process. Catal Rev - Sci Eng. 23, 265-278. DOI= 10.1080/03602458108068078.

[7] Miroliaei, A.R., Shahraki, F., Atashi, H., et al. 2012 Comparison of CFD results and experimental data in a fixed bed Fischer–Tropsch synthesis reactor. J Ind Eng Chem. 18, 1912-1920. DOI=doi:10.1016/j.jiec.2012.05.003.

[8] Fazlollahi, F., Sarkari, M., Zare, A., et al. 2012.Development of a kinetic model for Fischer–Tropsch synthesis over Co/Ni/Al2O3 catalyst. J Ind Eng Chem, 18, 1223-1232. DOI= doi:10.1016/j.jiec.2011.10.011.

[9] Geerlings, J.J.C., Wilson, J.H., Kramer G.J, et al. 1999. Fischer–Tropsch technology — from active site to Commercial process. Appl Catal A. 186, 27-40. DOI= Doi: 10.1016/S0926-860X (99)00162-3.

[10] Dry, M.E. 1996. Practical and theoretical aspects of the Catalytic Fischer-Tropsch process. Appl Catal A. 138, 319-344. DOI= doi: 10.1016/0926-860X (95)00306-1

[11] Park, N., Kim, J.R, Y Yoo, et al. 2014. Modeling of a Pilot-scale fixed-bed reactor for iron-based Fischer–Tropsch synthesis: Two-dimensional approach for optimal tube diameter. Fuel, 122, 229-235. DOI=doi:10.1016/j.fuel.2014.01.044.

[12] Woo K.J., H Kang S., Kim S.M, and et al. 2010. Performance of a slurry bubble column reactor for Fischer–Tropsch synthesis: Determination of optimum condition. Fuel Proc Tech. 91, 434-439. DOI= doi:10.1016/j.fuproc.2009.04.021.

[13] Mirzaei, A.A., Sarani, R., Azizi, H.R et al. 2015.Kinetics modeling of Fischer–Tropsch synthesis on the unsupported Fe-Co-Ni (ternary) catalyst prepared using co-precipitation procedure. Fuel. 140, 701-710. DOI=doi:10.1016/j.fuel.2014.09.093.

[14] Mirzaei, A.A., Shirzadi, B., Atashi, H., et al. 2012. Modeling and operating conditions optimization of Fischer–Tropsch synthesis in a fixed-bed reactor. J Ind Eng Chem. 18, 1515-1521. DOI= doi:10.1016/j.jiec.2012.02.013.

[15] Jothimurugesan, K.J., G Goodwin, J.r., et al. 2000 Development of Fe Fischer–Tropsch catalysts for slurry bubble column reactors. Catal Today. 58, 335-344. DOI= doi: 10.1016/S0920-5861(00)00266-2.

[16] Lox ES, Marin GB, de Graeve E, et al. 1988 Characterization of a promoted precipitated iron catalyst for Fischer-Tropsch synthesis. App Catal A. 40, 197 218.DOI= doi: 10.1016/S0166-9834(00)80438-8.

[17] Prakash A. 1994. On the effects of syngas composition and water-gas-shift reaction rate on FT synthesis over IRON based catalyst in a slurry reactor. Chem Eng. Commun. 128, 143-158. DOI=10.1080/00986449408936242.

[18] Zimmerman, W.H., Ph.D. Thesis, TAMU, America, 1990.

[19] van der Laan, G.P., Beenackers, A.A.C.M. 1999.Kinetics and Selectivity of the Fischer–Tropsch Synthesis: A Literature Review. Catal Rev - Sci Eng. 41, 255-318.

[20] Nakhaei Pour, A., Kamali Shahri, M., Zamani, Y., et al. 2008. Deactivation studies of bifunctional Fe-HZSM5 catalyst in Fischer-Tropsch process. J Nat Gas Chem. 17, 242-248. DOI= doi: 10.1016/S1003-9953(08)60058-4

[21] Nakhaei Pour, A., Zamani, Y., Tavasoli, A., et al. 2008. Study on products distribution of iron and iron–zeolite catalysts in Fischer–Tropsch synthesis. Fuel. 87, 2004-2012. DOI= doi:10.1016/j.fuel.2007.10.014.

[22] Nakhaei Pour, A., Kamali Shahri, M., Bozorgzadeh,H.R, et al. 2008. Effect of Mg, La and Ca promoters on the structure and catalytic behavior of iron-based catalysts in Fischer–Tropsch synthesis. Appl Catal A, 348, 201-208. DOI= doi:10.1016/j.apcata.2008.06.045.

[23] Li, S., Li, A., Krishnamoorthy, S., et al. 2001. Effects of Zn, Cu, and K Promoters on the Structure and on the Reduction, Carburization, and Catalytic Behavior of Iron-Based Fischer–Tropsch Synthesis Catalysts. Catal. Letters, 77, 197-205.

[24] Yang, J., Sun, Y., Tang, Y., et al. 2006. Effect of magnesium promoter on iron-based catalyst for Fischer–Tropsch synthesis. J Mol Catal A. 245, 26-36. DOI= doi:10.1016/j.molcata.2005.08.051

[25] Tao, Z., Yang, Y., Zhang, C., et al. 2006. Effect of calcium promoter on a precipitated iron–manganese catalyst for Fischer–Tropsch synthesis. Catalysis Commun. 7, 1061-1066. DOI=doi:10.1016/j.catcom.2006.05.009.

[26] Yang, Y., Xiang, H.W., Xu, Y.Y., et al. 2004. Effect of Potassium promoter on precipitated iron-manganese catalyst for Fischer–Tropsch synthesis. Catal A G. 266,181-194. DOI= doi:10.1016/j.apcata.2004.02.018.

[27] Mansouri, M., Atashi, H., Farshchi Tabrizi, F., et al. 2013. Kinetics studies of nano-structured cobalt– manganese oxide catalysts in Fischer–Tropsch synthesis. J Ind Eng Chem, 19, 1177-1183. DOI=10.1016/j.jiec.2012.12.015.

[28] Soong, Y., Rao, V.U.S., Gormley, R.J. 1991. Temperature-programmed desorption study on manganeseiron catalysts. Appl Catal. 78, 97-108. DOI= 10.1016/0166-9834(91)80091-A.

[29] Kreitman, K.M., Baerns, M., Butt, J.B. 1987. Manganese-oxide-supported iron Fischer-Tropsch synthesis catalysts: Physical and catalytic characterization. J Catal. 105, 319-334. DOI= 10.1016/0021-9517(87)90061-3.

[30] Yang, Y., Xiang, H., Zhang, R., et al. 2005. A highly active and stable Fe-Mn catalyst for slurry Fischer– Tropsch synthesis. catal Today . 106, 170-175. DOI=10.1016/j.cattod.2005.07.127

[31] Yang, Y., Xiang, H.W., Tian, L, et al. 2005. Structure and Fischer–Tropsch performance of iron–manganese catalyst incorporated with SiO2. Appl Catal A G, 284, 105-122. DOI= doi:10.1016/j.apcata.2005.01.025.

[32] Herranz, T., Rojas, S., Perez-Alonso, F.J, et al. 2006. Hydrogenation of carbon oxides over promoted Fe–Mn catalysts prepared by the micro emulsion methodology.Appl Catal A G. 311, 66-75. DOI=doi:10.1016/j.apcata.2006.06.007.

[33] Zhang, C.H., Yang, Y., Tang, B.T., et al. 2006. Study of an iron- manganese Fischer–Tropsch synthesis catalyst promoted with copper. J Catal. 237, 405-415. DOI=doi:10.1016/j.jcat.2005.11.004.

[34] Rados, N., Al-dahhan, M.H., Dudukovic, M.P. 2003. Modeling of the Fischer–Tropsch synthesis in slurry bubble column reactors. Catal Today. 79–80, 211-218. DOI= doi: 10.1016/S0920-5861(03)00007-5.

[35] Sharma, B.K., Sharmaa, M.P., Kumar, Roya S., et al.1998. Fischer–Tropsch synthesis with Co/SiO2–Al2O3 catalyst and steady-state modeling using artificial neural networks. Fuel 77, 1763-1768. DOI= doi: 10.1016/S0016-2361(98)00110-0.

[36] Myshkin, N.K., Kwon OK., Grigoriev, A.Y, et al. 1997.

Classification of wear debris using a neural network. Wear. 203-204, 658-662. DOI= doi: 10.1016/S0043-1648(96)07432-7.

[37] Schooling, J.M., Brown, M., Reed, P.A.S. 1999. An example of the use of neural computing techniques in materials science—the modelling of fatigue thresholds in Ni-base super alloys. Sci Eng A. 260, 222-239.

[38] Renno, C., Petito, F., Gatto, A. 2015. Artificial neural network models for predicting the solar radiation as input of a concentrating photovoltaic system. Energy Convers Manage. 106, 999–1012 DOI= doi:10.1016/j.enconman.2015.10.033.

[39] Mikulandric, R., Loncar, D., Böhning, D., et al. 2014. Artificial neural network modelling approach for a biomass gasification process in fixed bed gasifiers. Energy Convers Manage. 87, 1210–1223. DOI=doi:10.1016/j.enconman.2014.03.036.

[40] Yuhong, Z., Wenxin, H. 2009. Application of artificial neural network to predict the friction factor of open channel flow. Nonlinear Sci Numer Simulat, 14, 2373-2378.

[41] Adib H, Haghbakhsh R, Saidi M, et al. 2013. Modeling and optimization of FischereTropsch synthesis in the presence of (III)/Al2O3 catalyst using artificial neural networks and genetic algorithm. J nat Gas Sci Eng. 10, 14-24.DOI= doi:10.1016/j.jngse.2012.09.001.

[42] Tu, Y.L., Chang, T.J., Hsieh, C.I, et al. 2010. Artificial neural networks in the estimation of monthly capacity factors of WECS in Taiwan. Energy Convers Manage, 51, 2938–2946. DOI= doi:10.1016/j.enconman.2010.06.035.

[43] Xie, G.N., Wang, Q.W., Zeng, M, et al. 2007. Heat Transfer analysis for shell-and-tube heat exchangers with Experimental data by artificial neural networks approach. Appl Thermal Eng. 27, 1096-1104. DOI=doi:10.1016/j.applthermaleng.2006.07.036.

[44] Kurt, H., Atik, K., Ozkaymak, M., et al. 2008. Thermal performance parameters estimation of hot box type solar cooker by using artificial neural network. Int J Thermal Sci. 47, 192-200. DOI=doi:10.1016/j.ijthermalsci.2007.02.007.

[45] Wang, Y., Fan, W., Liu, Y., et al. 2008. Modeling of the Fischer–Tropsch synthesis in slurry bubble column reactors. Chem Eng Proc. 47, 222-228. DOI=doi:10.1016/j.cep.2007.02.011

Table 1. Experimental data for hydrocarbon products on Fe-Mn catalyst at inlet superficial gas velocity 0.2 m/s and different temperatures, pressures and H_2/CO ratios

Test. No	T(K)	P(Mpa)	H_2/CO	%CH_4	%diesel	%gasoline	%C_{21}^+
1	523	3	1	1.94	14.5	14.7	57.1
2	526	3	1	2.74	16.3	15.6	53.2
3	533	3	1	4.35	20.5	18.1	44
4	536	3	1	5.60	21.1	19.4	38.87
5	543	3	1	8.23	22.7	24.2	26.8
6	546	3	1	9.84	21.9	25.6	22.74
7	553	3	1	13.7	20.2	28.9	13.1
8	556	3	1	15.8	18.4	29	10.64
9	563	3	1	20.8	14.4	29.7	5.16
10	566	3	1	23.4	12.4	28.5	4.03
11	573	3	1	29.1	8.06	26.1	1.45
12	543	3	0.67	3.78	16.8	16.8	46.9
13	543	3	0.75	4.86	18.1	18.5	42.03
14	543	3	1.25	12.6	20.4	28.4	17.17
15	543	3	1.5	17	18.1	32.6	7.16
16	543	3	1.75	23.1	13.2	31.5	4.19
17	543	3	2	29.2	8.24	30.7	1.08
18	543	1.5	1	18.5	17.5	25.2	13.4
19	543	1.75	1	16	18.9	25.3	15.92
20	543	2	1	13.4	20.3	25.5	18.4
21	543	2.25	1	11.9	21.1	25.2	20.59
22	543	2.5	1	10.3	21.8	25	22.7
23	543	2.75	1	9.31	22.2	24.6	24.67
24	543	3.25	1.00	7.43	22.8	23.6	25.71
25	543	3.5	1.00	6.43	22.9	23	26.8

Table 2. Catalyst Properties

Catalyst Properties	Value
Particle density	1900Kg.m^{-3}
Thermal conductivity	1.7 $Wm^{-1}.K^{-1}$
Heat capacity	993j.$Kg^{-1}.K^{-1}$
Diameters of catalyst particle	80×10^{-6}m

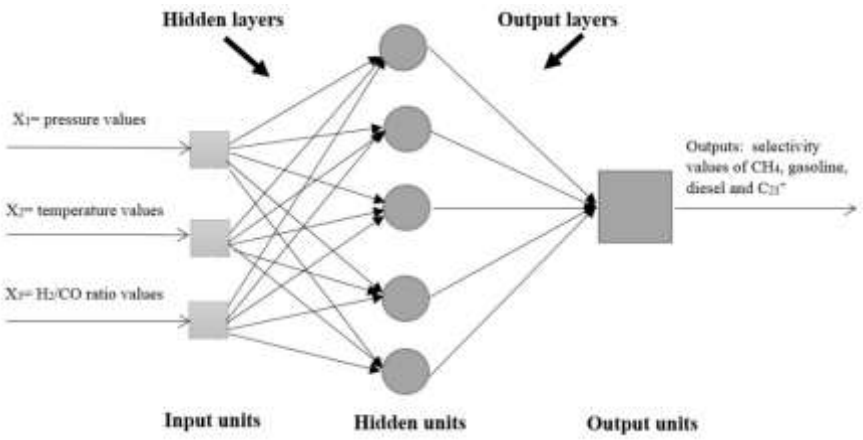

Fig.1. Structure of artificial neural network

Table 3. Calculated responses by artificial neural network for designed experimental condition

P(Mpa)	H_2/CO	T(K)	$\%CH_4$	%gasoline	%diesel	$\%C_{21}^+$
2.5	1.34	548	20.76	33.27	21.87	4.57
3.5	2	573	53.74	28.74	25.26	0
3.5	1.34	548	14.91	29.03	22.33	12.72
2.5	1.34	523	6.32	22.91	7.77	34.96
2.5	1.34	548	20.76	33.27	21.78	4.57
3.5	2	523	11.49	25.84	2.26	15.04
2.5	2	548	38.48	30.86	12.16	0
1.5	1.34	548	30.32	31.35	17.49	5.15
3.5	0.67	573	18.71	17.74	3.08	10.92
2.5	1.34	548	20.76	33.27	21.87	4.57
3.5	0.67	523	0	7.91	20.32	67.51
2.5	1.34	548	20.76	33.27	21.87	4.57
1.5	2	573	69.39	27.86	19.94	3.63
1.5	2	523	26.06	29.23	0.22	5.96
1.5	0.67	573	34.12	22.94	0	4.71
2.5	1.34	548	20.76	33.27	21.87	4.57
2.5	1.34	548	20.76	33.27	21.87	4.57
2.5	0.67	548	5.39	17.28	11.96	32.25
2.5	1.34	573	20.85	28.99	28.99	0
2.5	1.34	573	20.85	2.63	2.63	50.82

Table 4. Regression results obtained from neural network

Products	Training	Validation	Test	All
Diesel	0.997	0.997	0.996	0.991
Gasoline	0.999	0.997	0.996	0.996
C_{21}^{+}	0.999	0.999	1	0.999

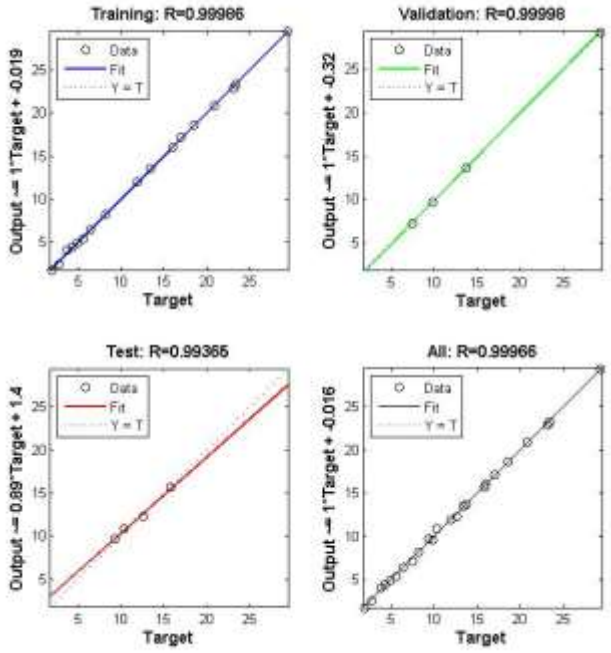

Fig.2.The regression graph obtained from neural network for CH_4

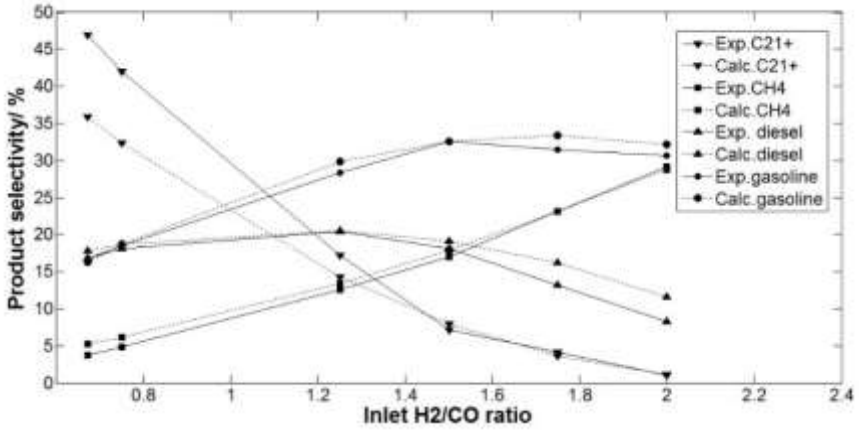

Fig.3. Compare calculated data with the experimental data at variant H_2/CO ratio

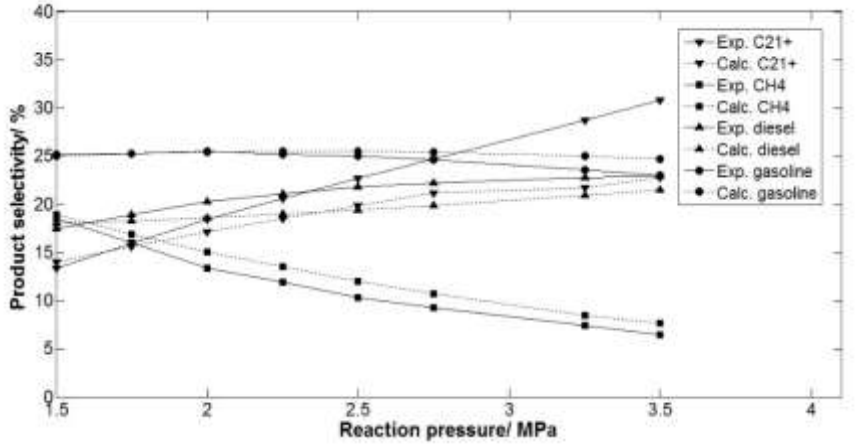

Fig.4. Comparison of calculated data with the experimental data at variant pressure

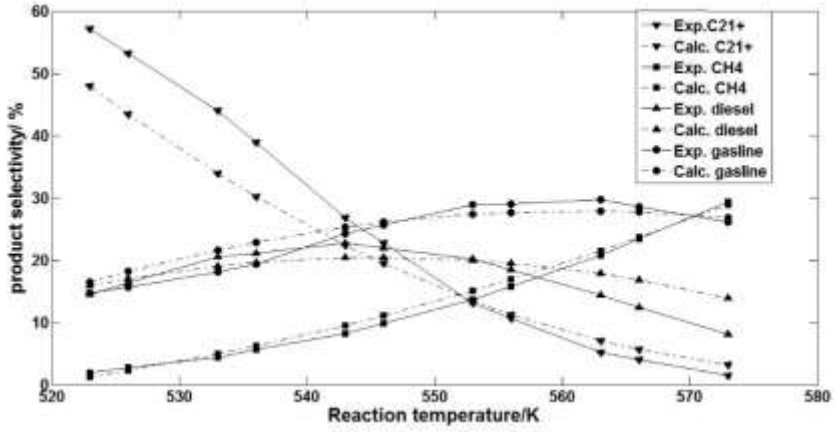

Fig.5. Comparison of calculated data with the experimental data at variant temperature

Table 5. Optimization results for products

	T(K)	P(Mpa)	H_2/CO ratio	Selectivity%
Maximization of S_{diesel}	559.87	3.5	1.64	25.03
Minimization of S_{diesel}	523	2.01	2	0
Maximization of $S_{gasoline}$	545.22	1.5	1.88	37.84
Minimization of $S_{gasoline}$	523	3.24	0.67	8.48
Maximization of S_{C21^+}	523	3.24	0.67	67.08
Minimization of S_{C21^+}	0	546,74	1.5	2
Maximization of S_{CH4}	523	1.5	2	67.05
Minimization of S_{CH4}	523	3.04	1.02	0

Table 6. Basic and modified selectivity model and statistical indicators of C_{21^+}

C_{21^+} basic selectivity model=4521.1+74.37*P-405.32*N-15.17*T-3.28*P*N+0.64*N*T-0.57*P^2+15.01*N^2+0.01*T^2

C_{21^+} modified selectivity model=4420.55+71.51*P–404.02*N–14.79*N–3.28*P*N-0.11*P*T+0.64*N*T+14.52*N^2+0.01*T^2

Indicator statistical of basic model	P-value	Model	P	N	T	P*N	P*T	N*T	P^2	N^2	T^2
		<0.0001	0.005	<0.0001	<0.0001	0.08	0.027	<0.0001	0.77	0.006	0.001
	R-squared			Adj-R-squared			C.V.%			Standard deviation	
	0.98			0.97			23.41			3.17	
Indicator statistical of modified model	P-value	Model		P	N	T	P*N	P*T	N*T	N^2	T^2
		<0.0001		0.003	<0.0001	<0.0001	0.067	0.02	<0.0001	0.003	0.0008
	R-squared		Adj-R-squared			C.V.%			Standard deviation		
	0.98		0.97			22.42			3.04		

P is pressure in (MPa), T is temperature in (K) and N is H_2/CO ratio

Table 7. Basic and modified selectivity model and statistical indicators of CH_4

CH_4 basic selectivity model=1178.26+21.80*P–142.50*N–4.67*T–1.91*P*N-0.059*P*T+0.28*N*T+1.31*P^2

CH_4 modified selectivity model=1415.68+25.83*P-150.27*N-5.54*T-0.059*P*T+0.28*N*T+5.96*N^2+0.0055*T^2

Indicator statistical of basic model	P-value	Model	P	N	T	P*N	P*T	N*T	P^2	N^2	T^2
		<0.0001	<0.0001	<0.0001	<0.0001	0.048	0.025	<0.0001	0.201	0.05	0.012
	R-squared			Adj-R-squared			C.V.%		Standard deviation		
	0.99			0.99			6.6		1.59		
Indicator statistical of modified model	P-value	Model	P	N	T	P*T	N*T	N^2	T^2		
		<0.0001	<0.0001	<0.0001	<0.0001	0.047	<0.0001	0.028	0.007		
	R-squared			Adj-R-squared			C.V.%		Standard deviation		
	0.99			0.98			7.84		1.89		

P is pressure in (MPa), T is temperature in (K) and N is H_2/CO ratio

Table 8. Basic and modified selectivity model and statistical indicators of gasoline

Gasoline basic selectivity model = -2644.39+20.41*P+171.42+9.08*T–0.49*P*N-0.03*P*T-0.21*N*T–0.64*P^2–15.34*N^2–0.78*T^2											
Gasoline modified selectivity model = -2715.33+171.66*N+9.43*T–0.21*N*T–15.89*N^2–0.0082*T^2											
Indicator statistical of basic model	P-value	model	P	N	T	P*N	P*T	N*T	P^2	N^2	T^2
		<0.0001	0.517	<0.0001	0.0003	0.689	0.35	0.001	0.641	0.0005	0.004
	R-squared			Adj-R-squared				C.V.%		Standard deviation	
	0.96			0.93				8.57		2.24	
Indicator statistical of modified model	P-value	Model		N	T		N*T	N^2		T^2	
		<0.0001		<0.0001	<0.0001		0.0002	<0.0001		0.0005	
	R-squared			Adj-R-squared			C.V.%		Standard deviation		
	0.96			0.94			7.87		2.06		

P is pressure in (MPa), T is temperature in (K) and N is H_2/CO ratio

Table 9. Basic and modified selectivity model and statistical indicators of diesel

Diesel basic selectivity model = -1767.77–11.68*P–275.13*N+7.15*T+0.14*P*N+0.01*P*T+0.58*N*T+1.11*P^2–15.29*N^2–0.72*T^2											
Diesel modified selectivity model = -1592.82+1.87*P–277.29*N+6.46*T+0.58*N*T-14.35*N^2–0.0065*T^2											
Indicator statistical of basic model	P-value	Model	P	N	T	P*N	P*T	N*T	P^2	N^2	T^2
		<0.0001	0.065	0.418	0.037	0.926	0.732	<0.0001	0.535	0.003	0.026
	R-squared			Adj-R-squared			C.V.%		Standard deviation		
	0.94			0.88			18.41		2.87		
Indicator statistical of modified model	P-value	Model		P	N	T	N*T	N^2	T^2		
		<0.0001		0.038	0.365	0.019	<0.0001	0.0007	0.014		
	R-squared			Adj-R-squared			C.V.%		Standard deviation		
	0.94			0.91			16.58		2.58		

P is pressure in (MPa), T is temperature in (K) and NisH_2/CO ratio

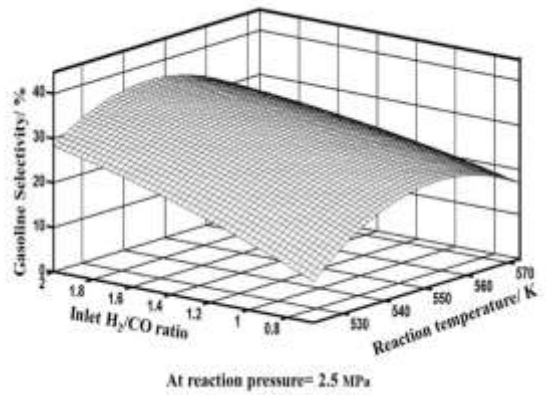

Fig. 6a

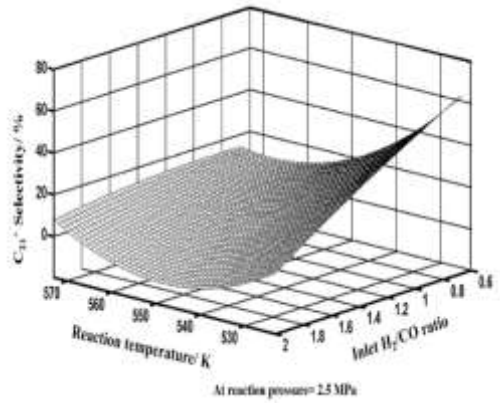

Fig.6b

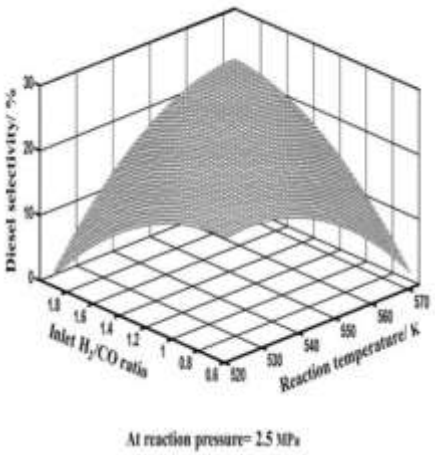

Fig.6c

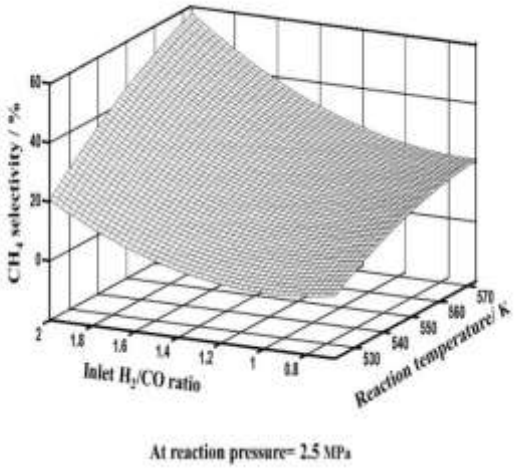

Fig.6d

Fig. 6. Variation of calculated selectivity of products as a function of temperature value and H_2/CO ratio value at P=2.5 MP

